

Effect of Liquid Crystal Structures on Photopolymerization-Induced Phase Separation Behavior as Determined from Simultaneous Resistivity and Turbidity Measurements

Sucheol Park, Sang Sub Lee, Jin Who Hong

Department of Polymer Science and Engineering, Chosun University, Gwangju, Korea

Abstract

Photopolymerization and phase separation behavior during the formation of polymer-dispersed liquid crystal (PDLC) were investigated by simultaneous resistivity and turbidity measurements. This method provides information on the rate and the degree of polymerization and liquid crystal phase separation. Using this experimental method, we investigated the effect of liquid crystal structures on photopolymerization and phase separation behavior during the process of PDLC formation.

Introduction

Polymer-dispersed liquid crystal (PDLC) is a polymer/liquid crystal (LC) composite and used in switchable glass and imaging technologies due to its attractive intrinsic electrooptical characteristics. PDLC is normally made by photopolymerization-induced phase separation in a homogeneous mixture of prepolymer and LC, with prepolymer curing and phase separation resulting in the formation of nematic microdomains.

Several studies have investigated the relationship between PDLC morphology and electrooptical performance characteristics such as the scattering when switched off, the transmittance when switched on, and the switching voltage itself. Because the morphology of PDLC is strongly influenced by both the photopolymerization and phase separation processes, it is important to understand their underlying mechanisms. Experimental methods introduced to allow simultaneous examination of the polymerization and the LC phase separation have utilized real-time FTIR spectroscopy and photo-differential scanning calorimetry (photo-DSC) combined with a turbidity accessory.

The polymerization and phase separation are greatly influenced by the physical and chemical properties of LCs and prepolymers, such as solubility parameters and the diffusion coefficient. Many studies have investigated the use of E7 as a nematic LC mixture and NOA65 as prepolymer. E7 is a eutectic LC mixture consisting of several cyanobiphenyl (CB) and cyanoterphenyl compounds. Despite the widespread use of E7, the phase separation behavior of individual components has rarely been studied. Knowledge of this behavior during the polymerization process would improve the understanding of the PDLC process and result in the formulation of improved LC mixtures.

Here, we describe an experimental method for monitoring the photopolymerization and phase separation process of PDLC based on simultaneous resistivity and transmittance measurements. This method was used to investigate the effect of the chemical structure of the LC component on photopolymerization and phase separation behavior.

Experimental

Materials

A formulated UV curable adhesive, NOA65 (Norland Products) was used as a prepolymer, which consists of a mixture of trimethylolpropane trithiol, a tetrafunctional allyl ether formed from the reaction of trimethylolpropane diallyl ether and isophorone diisocyanate and benzophenone (BP) as a photoinitiator. To investigate the effects of the chemical structure of LC compounds, we selected four LC compounds with different ring structures and alkyl groups of different lengths; 4-n-pentyl-4'-cyanobiphenyl (5CB), 4-n-heptyl-4'-cyanobiphenyl (7CB), 4-trans-pentyl cyclohexyl cyanobenzene (5PCH) and 4-trans-heptyl cyclohexyl cyanobenzene (7PCH). The PDLC formulations comprised mixtures of NOA65 and each LC compound at a 1:1 weight ratio.

Measurements

The experimental setup is illustrated in Fig. 1. A PDLC cell was prepared by sandwiching the sample mixture between two ITO coated glass (50 x 30mm²) with thickness of 20μm using spacers. A resistivity meter (Megaresta H0709, Shishido Electrostatic) was used to measure the resistivity of the PDLC cell. A halogen lamp (Avalight-HAL, Avantes) and CCD detector (Avastpec 2048, Avantes) coupled to a fiber-optic cable was used to measure the transmittance of the PDLC cell. Photopolymerization was initiated using a UV lamp (B-14N, Spectronics) producing an intensity of 1.6mW/cm² at 365nm. All measurements were performed at room temperature.

Photo-differential scanning calorimetry (photo-DSC, Thermal Analysis TA5000) was used to investigate the photopolymerization behavior. Photo-DSC measurements were performed under a nitrogen atmosphere. The photopolymerization was initiated with the same UV lamp used in the resistivity-transmittance measurements.

UV spectra of the LC compounds and benzophenone (photo-initiator) were measured using a spectrophotometer (Cary500scan, Varian).

Scanning electron microscopy (SEM, JSM-6490, JEOL) was used to examine the PDLC morphology. The PDLC samples were freeze fractured, soaked in hexane for 24h to remove the liquid crystals from the exposed surface, and placed under vacuum chamber for 24h to remove the solvent.

Results and discussion

Photopolymerization is usually monitored using photo-DSC, FTIR spectroscopy, and dielectric and rheological analysis. The photopolymerization process can also be monitored by measuring the electrical conductivity, which consists of dipolar and ionic components. The dipolar component arises from rotational motion of molar dipoles and the ionic component arises from the diffusion of ionic impurities that may form during synthesis. As the polymerization progresses, the electrical effects due to these conducting species reduces. The relation between conductivity and resin viscosity can be expressed as

$$\text{viscosity} \propto \text{resistivity} \propto 1/\text{conductivity} \quad (1)$$

Fig. 2 shows the photo-DSC thermograms of the mixtures of NOA65 and LC compounds investigated in this study, which indicates that photopolymerization behavior differs significantly between CBs and PCHs. The PCHs show faster photopolymerization and earlier termination than CBs. For LC compounds having the same ring structure, a longer alkyl group causes slightly earlier and faster photopolymerization. Parameters characterizing the photo-DSC thermograms are listed in Table 1. The time at peak maximum, which is related to the rate of photopolymerization, is much earlier for PCHs than for CBs. The enthalpy, which is related to the percentage conversion of NOA65, is higher for PCHs than for CBs. The slower photopolymerization and lower conversion for CBs compared with PCHs can be thought by the UV shield and dilution effect. To investigate the UV shield effect, the irradiation spectrum of UV lamp in this study and the absorption spectra of 5PCH, PCB, and BP were measured and shown in Fig. 3. UV lamp emits UV light over the range 300~400nm, with a peak at 365nm. While 5CB absorbs the UV light from the lamp over the range 300~340nm, 5PCH exhibits no absorption. The UV spectra of 7PCH and 7CB are almost same as 5PCH and 5CB, respectively. Given that the CBs absorbs or shields the UV light over the range 300~340nm from the lamp, CBs reduce the photopolymerization and conversion of NOA65. However, the shield effect does not seem to be the major factor when considering the amount of shielded light by CBs, only 10% to the total UV energy.

The photopolymerization of NOA65 propagates by the addition of thiyl radicals to ene monomers. The addition reaction in a homogeneous mixture of LCs and NOA65 is restricted by LC molecules (dilution effect), and hence the photopolymerization rate might be higher if LC molecules separate into droplets earlier. If PCHs separate earlier than CBs, PCHs would result in the earlier photopolymerization of NOA65 compared with CBs. This is evident from the turbidity data in Fig. 4b.

Fig.4a shows the resistivity of PDLC cells as a function of irradiation time. As the polymerization reaction of NOA65 progresses, the resistivity increases in accordance with the viscosity increase. Similar to the photo-DSC thermograms, the resistivity increases much faster for PCHs than for CBs. Moreover, the resistivity increases faster and reaches a higher level when the alkyl group is longer. The resistivity results coincide well with the photo-DSC results, indicating that resistivity analysis can be used to monitor the photopolymerization process of PCLD. However, while the enthalpy is in the order $7PCH > 5PCH > 7CB \approx 5CB$, the final resistivity is in the order $7PCH > 5PCH > 7CB > 5CB$. This difference can be explained by considering the meaning of these two parameters. The enthalpy measured by a photo-DSC thermogram arises from the heat released by the reaction of NOA65, and is directly associated with the conversion of NOA65 regardless of the phase separation of LC molecules. However, the resistivity arises from the bulk viscosity of PCLD, which is associated with the plasticization effect of LC molecules as well as the conversion of NOA65. The LC molecules dissolved in the polymer matrix act as a plasticizer and reduce the viscosity of PDLC. According to this approach, the differences can be explained as follows:

- 1) Despite the percentage conversion of NOA65 reaching the same level for the NOA65/5CB and NOA65-7CB systems, the presence of more 5CB molecules remaining in the matrix results in greater plasticization compared to 7CB. This is evident from the turbidity data in Fig. 4.
- 2) While the conversion of NOA65 is approximately 10% higher for the NOA65-7PCH system than for the NOA65-5PCH system, the difference in final resistivity is very small. In contrast to CB, 5PCH and 7PCH can be significantly separated to form droplets, which can be crudely estimated from the turbidity data. Therefore, the 10% difference in the final conversion does not significantly affect the final resistivity.

Fig. 4b shows the transmittance as a function of irradiation time. The turbidity of 5CB did not change, which indicates that 5CB molecules cannot be separated sufficiently from the matrix to form droplets to scatter the light, despite significant conversion of NOA65. The transmittance of 7CB decreases from 60 sec and its final transmittance is still high, indicating that some of the 7CB molecules are separated from the matrix to form droplets. However, the amount and/or size of droplets formed are too small to markedly scatter the light. In contrast, the transmittance of PCHs changes earlier and reaches a much higher level than CBs. This behavior clearly shows that the PCH

molecules are easily separated during the photopolymerization process. Finally, the transmittance of 7PCH decreases earlier and reaches a higher level than that of 5PCH.

The resistivity and enthalpy values at the initiation of turbidity are listed in Table 2. Turbidity is initiated at 15 sec and 18 sec for 7PCH and 5PCH, respectively, at which times the enthalpies are 67.0J/g and 56.0H/g. It is interesting that although 7PCH requires a higher conversion of NOA65 to form droplets than 5PCH, 7PCH reaches the required conversion faster than does 5PCH. On the other hand, 7CB requires a much higher conversion to form droplets compared with PCHs.

According to the photo-DSC and resistivity results, the polymerization reactions terminate at about 60 sec for PCHs and 120 sec for CBs. The transmittance values do not change after these times. The results also indicate the following:

- 1) The photopolymerization of NOA65 is greatly restricted by CB molecules, and the gelation is delayed due to both restricted photopolymerization and the plasticization of CB molecules dissolved in matrix.
- 2) At the gel point, phase separation of LC molecules and droplet growth is terminated because the mobility of LC molecules greatly reduced.

The turbidity data can be the evidence of the dilution effect discussed in the photo-DSC results. The PCH molecules separate into droplets earlier and more readily than CB, it results in the earlier photopolymerization of NOA65. This mechanism would also explain the second exothermic peaks in the photo-DSC thermograms of 7PCH, 5PCH, and 7CB. The time of the second exothermic peak coincide well with the initiation of turbidity. Therefore, the second exothermic peak appears to be originated from the accelerated photopolymerization due to the LC phase separation. However, the turbidity data indicate that 5CB cannot be separated sufficiently from the matrix to form droplets, resulting in no second exothermic peak in its photo-DSC thermogram.

Fig. 5 shows the SEM micrographs of the PDLC samples. As expected in the resistivity and turbidity data, 5CB shows no droplet while 7CB shows small droplets. The PCHs show distinct and larger droplets compared with CBs. The droplet size of 7PCH is much larger than that of 5PCH, which results from the earlier and higher level of phase separation of 7PCH than that of 5PCH.

Conclusions

The photopolymerization and phase separation behavior during the process of PDLC formation were investigated by simultaneous resistivity and turbidity measurements. The photopolymerization behavior as determined from resistivity measurements was compared with data from photo-DSC

measurements. While the photo-DSC data only reflect the reaction behavior of polymer components, the resistivity provides information on the degree of polymerization and LC phase separation.

The effect of LC structure on the photopolymerization and phase separation behavior was also investigated. The phase separation behavior differed significantly between CB and PCH, with PCH being phase separated much more easily than CB. These differences in phase separation characteristics, resulted in very different photopolymerization behaviors, with the photopolymerization rate and conversion both being much higher for PCH than for CB.

References

1. Doane JW, Vaz NA, Wu BG, Zumer S. *Appl Phys Lett* 1986; 48(4): 269-271
2. Drzaic PS, Gonzales AM, Konynenburg PV. *Proc. SPIE* 1994; 2175: 148-157
3. Lampert CM. *Materialstoday* 2004; March: 28-35
4. Amundson K, Blaaderen AV, Wiltzius P. *Phys Rev E* 1997; 55(2): 1646-1654
5. Carter SA, GeGrange JD, White W, Boo J, Wiltzius P. 1997; 81(9):5992-5999
6. Nastal E, Zuranska E, Mucha M. *J Appl Polym Sci* 1999; 71(33): 455-463
7. Han JW. *J Korean Phys Soc* 2000; 36(3): 156-163
8. Bhargava R, Wang SQ, Koenig JL. *Macromolecules* 1999; 32(26): 8982-8988
9. Bhargava R, Wang SQ, Koenig JL. *Macromolecules* 1999; 32(26): 8989-8995
10. Kloosterboer JG, Serbutoviez C, Touwslager FJ. *Polymer* 1996; 37(26): 5937-5942
11. Smith GW. *Mol Cryst Liq Cryst* 1991; 196(1): 89-102
12. Smith GW. *Mol Cryst Liq Cryst* 1994; 239(1): 63-85
13. Lovinger AJ, Amundson K, Davis DD. *Chem Mater* 1994; 6(10): 1726-1736
14. Amundson K. *Phys Rev E* 1996; 53(3): 2412-2422
15. Challa SR, Wang SQ, Koenig JL. *Appl Spectrosc* 1997; 51(1): 10-16
16. Hoyle CE, Lee TY, Roper T. *J Polym Sci Part A* 2004; 42(21): 5301-5338
17. Cook WD, *J Polym Sci Part A* 1993 ; 31(4) : 1053-1086
18. Roussel F, Buisine JM. *Liq Cryst* 1998; 24(4): 555-561
19. Cho JD, Ju HT, Hong JW, *J Polym Sci Part A* 2005; 43(3): 658-670
20. Pethrick RA, Hayward D. *Prog. Polym Sci* 2002; 27(9): 1983-2017
21. Zahouily, Decker C, Kaisersberger E, Gruener M. *RadTech Technical Proceedings* 2004:
22. Cho JD, Han ST, Hong JW. *Polymer Testing* 2007; 26(1): 71-76

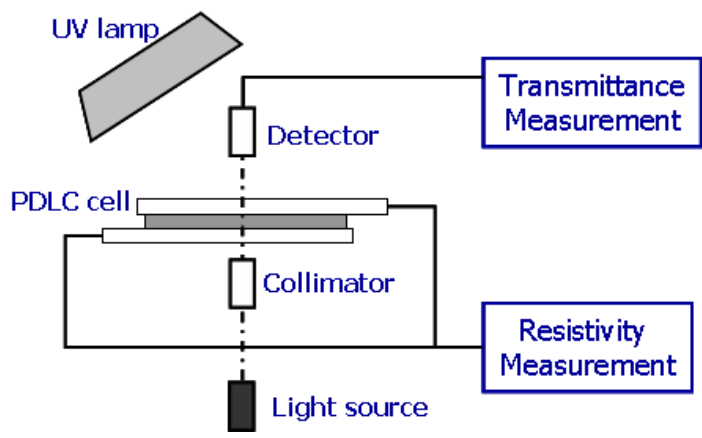


Figure 1. Experimental setup for simultaneously measuring the transmittance and resistivity of a PDLC cell during photopolymerization.

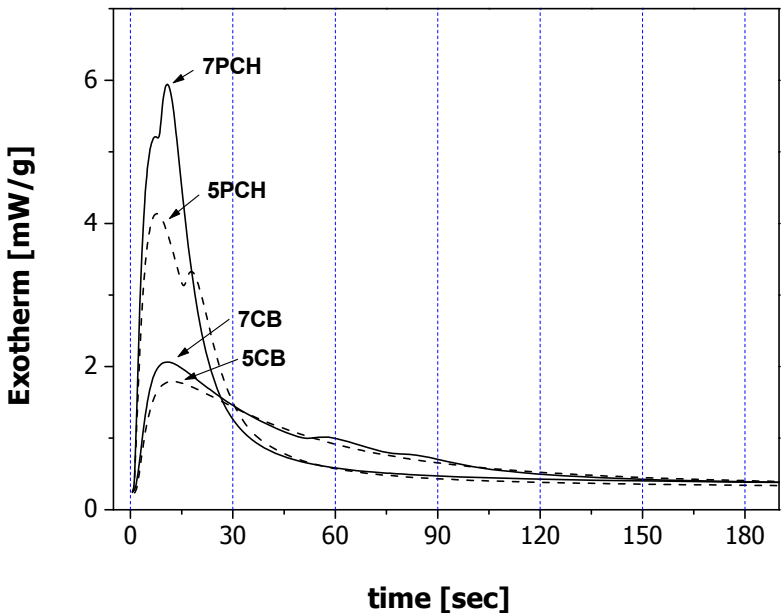


Figure 2. Photo-DSC thermograms of mixtures of NOA65 and LC compounds.

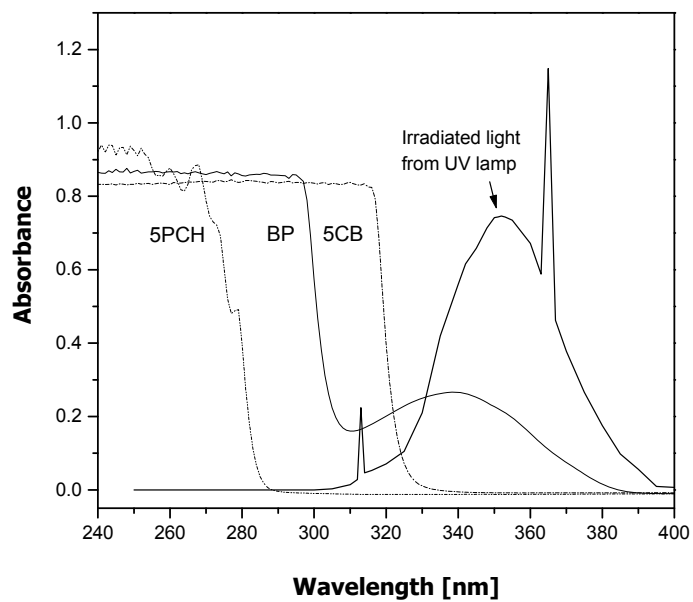


Figure 3. Irradiation spectrum of UV lamp in this study and absorption spectra of 5CB, 5PCH, and benzophenone.

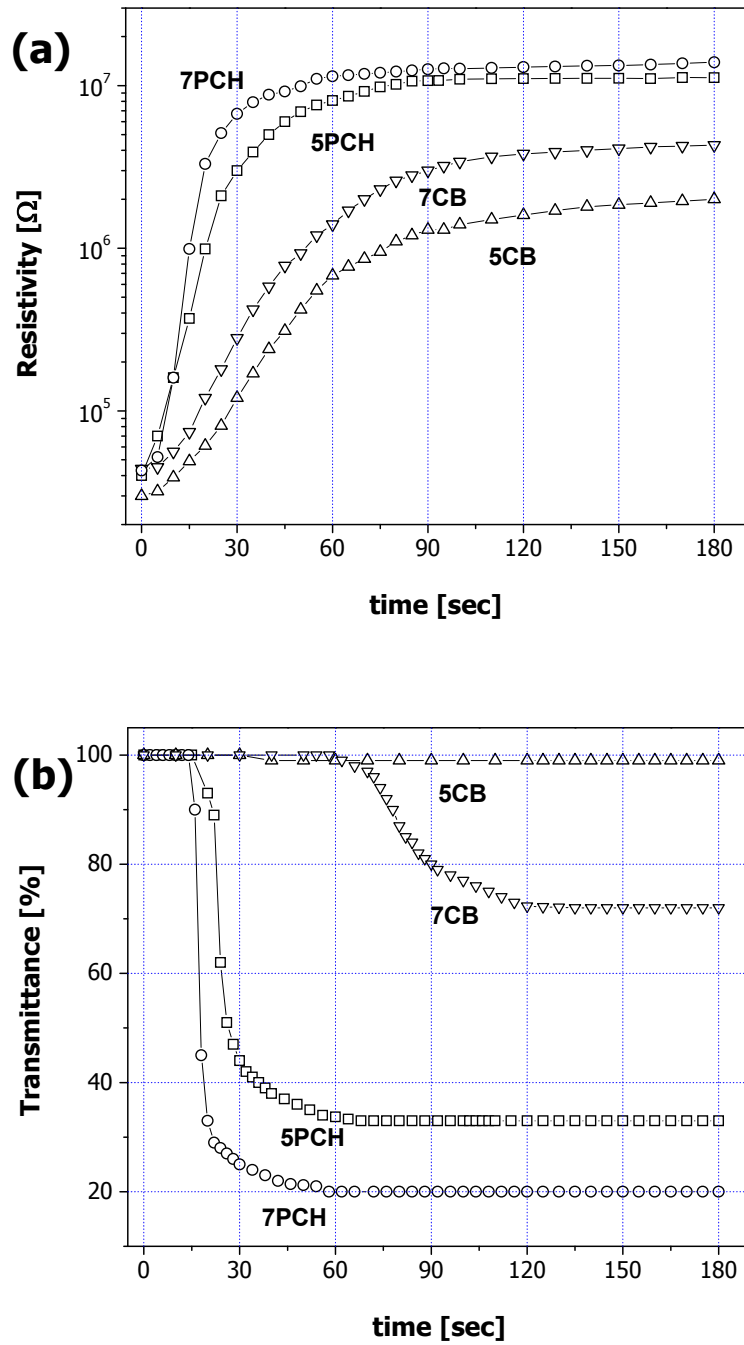


Figure 4. (a) Resistivity of PDLC cells as a function of photopolymerization time.
 (b) Transmittance of PDLC cells as a function of photopolymerization time.

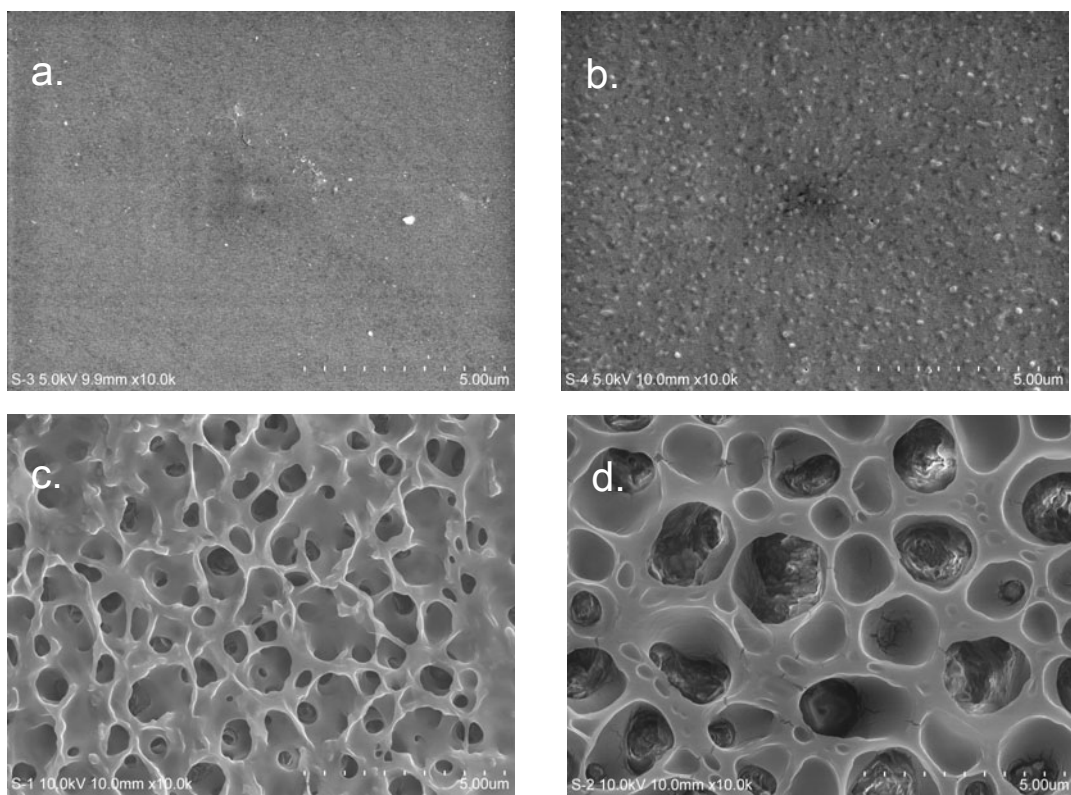


Figure 5. SEM micrographs of PDLCs with different LC compounds: (a) NOA65/5CB, (b) NOA65/7CB, (c) NOA65/5PCH, and (d) NOA65/7PCH.

Table 1. Parameters of NOA65 and LC compounds from photo-DSC thermograms.

	$t_{\max 1}$ (s)	$t_{\max 2}$ (s)	$w_{1/2}$ (s)	ΔH (J/g)
5CB + NOA65	12.3	-	58.4	180.3
7CB + NOA65	10.7	57.9	45.4	179.9
5PCH + NOA65	7.8	17.7	22.9	198.8
7PCH + NOA65	7.3	10.7	16.4	222.3

$t_{\max 1}$: time at first peak maximum

$t_{\max 2}$: time at second peak maximum

$w_{1/2}$: full width at half maximum

Table 2. Time (t_{turb}), resistivity (R_{turb}) and enthalpy (ΔH_{turb}) at the initiation of turbidity.

	t_{turb} (s)	R_{turb} (Ω)	ΔH_{turb} (J/g)
5CB + NOA65	-	-	-
7CB + NOA65	66	1.7×10^6	82.0
5PCH + NOA65	18	7.4×10^5	56.8
7PCH + NOA65	15	9.9×10^5	67.0